

# HC<sub>3</sub>N Observations of Nearby Galaxies \* ★ (Research Note)

Xue-Jian Jiang<sup>1,5</sup>, Jun-Zhi Wang<sup>2</sup>, Yu Gao<sup>1,5</sup>, and Qiu-Sheng Gu<sup>3,4,5</sup>

<sup>1</sup> Purple Mountain Observatory & Key Laboratory for Radio Astronomy, Chinese Academy of Sciences, 2 West Beijing Road, Nanjing 210008, China; Email: xjiang@pmo.ac.cn

<sup>2</sup> Shanghai Astronomical Observatory, Chinese Academy of Sciences, 80 Nandan Road, Shanghai 200030, China

<sup>3</sup> School of Astronomy and Space Sciences, Nanjing University, Nanjing 210093, China

<sup>4</sup> Key Laboratory of Modern Astronomy and Astrophysics (Nanjing University), Ministry of Education, Nanjing 210093, China

<sup>5</sup> Collaborative Innovation Center of Modern Astronomy and Space Exploration, Nanjing 210093, China

Received 2016 month day; accepted 2016 month day

## ABSTRACT

**Aims.** We aim to systematically study the properties of the different transitions of the dense molecular gas tracer HC<sub>3</sub>N in galaxies.

**Methods.** We have conducted single-dish observations of HC<sub>3</sub>N emission lines towards a sample of nearby gas-rich galaxies. HC<sub>3</sub>N( $J=2-1$ ) was observed in 20 galaxies with Effelsberg 100-m telescope. HC<sub>3</sub>N( $J=24-23$ ) was observed in nine galaxies with the 10-m Submillimeter Telescope (SMT).

**Results.** HC<sub>3</sub>N 2-1 is detected in three galaxies: IC 342, M 66 and NGC 660 ( $> 3\sigma$ ). HC<sub>3</sub>N 24-23 is detected in three galaxies: IC 342, NGC 1068 and IC 694. This is the first measurements of HC<sub>3</sub>N 2-1 in a relatively large sample of external galaxies, although the detection rate is low. For the HC<sub>3</sub>N 2-1 non-detections, upper limits ( $2\sigma$ ) are derived for each galaxy, and stacking the non-detections is attempted to recover the weak signal of HC<sub>3</sub>N. But the stacked spectrum does not show any significant signs of HC<sub>3</sub>N 2-1 emission. The results are also compared with other transitions of HC<sub>3</sub>N observed in galaxies.

**Conclusions.** The low detection rate of both transitions suggests low abundance of HC<sub>3</sub>N in galaxies, which is consistent with other observational studies. The comparison between HC<sub>3</sub>N and HCN or HCO<sup>+</sup> shows a large diversity in the ratios between HC<sub>3</sub>N and HCN or HCO<sup>+</sup>. More observations are needed to interpret the behavior of HC<sub>3</sub>N in different types of galaxies.

**Key words.** galaxies: active – galaxies: ISM – galaxies: evolution – ISM: molecules

## 1. Introduction

Molecular lines play an essential role in our understanding of star formation activity and galaxy evolution. With molecular lines of different species and their different transitions, not only the chemical composition of the interstellar medium can be investigated, but other important physical parameters, such as temperature, pressure, density, and non-collisional pumping mechanism can be derived as well (e.g., Henkel et al. 1991; Evans 1999; Fukui & Kawamura 2010; Meier & Turner 2012; Meier et al. 2014). New facilities providing wide band and highly sensitive instruments are making weak line surveys and multi-species analysis feasible, and the detections and measurements of a variety of species, are helping us to reveal the gas components of galaxies, and how their abundances, densities, ratios reflect the radiative properties of galaxies. Multi-species, multi-transition molecular lines can be combined to diagnose the evolution stage of galaxies (Baan et al. 2014), because different species are sensitive to different physical environments, such

as photo dissociation regions (PDRs) dominated by young massive stars, X-rays dominated regions (XDRs) induced by active galactic nucleus (AGNs), and shock waves by cloud-cloud collisions (Aladro et al. 2011; Greve et al. 2009; Aladro et al. 2011; Costagliola et al. 2011; Viti et al. 2014).

One of the interstellar species that benefits from the upgraded facilities is cyanoacetylene (HC<sub>3</sub>N). HC<sub>3</sub>N was firstly detected in 1971 at 9.0977 GHz ( $J=2-1$ ) in the Galactic star forming region Sgr B2 (Turner 1971). The critical density of HC<sub>3</sub>N is comparable to the widely-used dense gas tracer HCN and can also trace dense molecular gas around star forming sites. HC<sub>3</sub>N has been detected in many star formation regions in the Milky Way with several transitions from centimeter to sub-millimeter (e.g., Suzuki et al. 1992). Due to the small rotational constant ( $\sim 1/13$  of CO), there are many closely spaced rotational transitions of HC<sub>3</sub>N (separated by only 9.1 GHz) at centimeter and millimeter wavelengths, and its levels are very sensitive to the changes in excitation (Meier & Turner 2012). This makes it easier to conduct multi-transition observations of HC<sub>3</sub>N lines than other dense molecular gas tracers, and can help better understand the excitation conditions of star forming regions. In contrast, the high- $J$  lines of other dense molecular gas tracers such

\* Based on observations with the 100-m telescope of the MPIfR (Max-Planck-Institut für Radioastronomie) at Effelsberg, and the Submillimeter Telescope (SMT). The SMT is operated by the Arizona Radio Observatory (ARO), Steward Observatory, University of Arizona.

as HCN and HCO<sup>+</sup> are at very high frequencies, thus it is difficult to observe them with ground-based telescopes. Another advantage of using HC<sub>3</sub>N lines is that HC<sub>3</sub>N is very likely optical thin even in low- $J$  transitions, due to the relatively low abundance (Irvine et al. 1987; Lindberg et al. 2011). And low opacity is important for accurate estimate of dense molecular gas mass for the study of relationship between dense molecular gas and star formation (Gao & Solomon 2004a,b; Wang et al. 2011; Zhang et al. 2014).

There have been efforts to detect HC<sub>3</sub>N in nearby galaxies, mainly in millimeter band. Observations suggest that HC<sub>3</sub>N is related to the warm, dense star forming gas, and is easily dissociated by UV radiation (Henkel et al. 1988; Costagliola et al. 2011; Costagliola et al. 2011; Lindberg et al. 2011; Aladro et al. 2011, Aladro et al. 2015). HC<sub>3</sub>N was found to be unusually luminous in NGC 4418, and it is attributed to its high abundance ( $10^{-7}$ ) as well as the intense radiation field in the dense and warm gas at the center of NGC 4418 (Aalto et al. 2007; Costagliola & Aalto 2010). Meier & Turner (2005, 2012); Meier et al. (2011, 2014) presented high resolution observations of HC<sub>3</sub>N ( $J=5-4$ ,  $10-9$ ,  $12-11$  and  $16-15$ ) of a few very nearby galaxies, and gave detailed analysis of the galactic structures and morphology that traced by HC<sub>3</sub>N and other dense gas tracers (HNC, HCN, CS, etc.). However, these results are still limited by their sample size, and the chemical process of HC<sub>3</sub>N is still unclear. Larger samples are still necessary for analyzing the properties of HC<sub>3</sub>N and how it relate to other galactic parameters. In this paper we present the first systematic survey of HC<sub>3</sub>N ( $J = 2 - 1$ ) and HC<sub>3</sub>N ( $J = 24 - 23$ ) in a relatively large sample of nearby galaxies. And the results are compared with the observations of HC<sub>3</sub>N in other transitions. The critical densities of HC<sub>3</sub>N  $J = 2 - 1$  and HC<sub>3</sub>N  $J = 24 - 23$  are about  $3 \times 10^3 \text{ cm}^{-3}$  and  $4 \times 10^6 \text{ cm}^{-3}$ , respectively. And the upper state energies ( $E_u$ ) of the two transitions are 1.3 K and 131 K, respectively (Costagliola & Aalto 2010).

## 2. Observations & Data reduction

We select nearby infrared bright galaxies (Sanders et al. 2003) with IRAS 60  $\mu\text{m}$  flux greater than 30 Jy and declination greater than  $-21^\circ$  to do this survey. It is not a complete but representative sample of infrared bright galaxies. The sample consists of 21 galaxies. Note that due to the different beam size of the two telescopes we used, the merger Arp 299 (IC 694 and NGC 3690) were observed as a single pointing by Effelsberg 100-m, while the two galaxies were observed separately by the SMT 10-m.

### 2.1. HC<sub>3</sub>N 2-1 observations with the Effelsberg 100-m

HC<sub>3</sub>N ( $J = 2 - 1$ ) ( $\nu_{\text{rest}} = 18.196 \text{ GHz}$ ) of 20 galaxies was observed with Effelsberg 100-m telescope in 2010. The Half Power Beam Width (HPBW) is  $46.5''$  at 18 GHz for the 100-m telescope. We used the 1.9 cm band receiver, 500 MHz bandwidth with 16384 channels correlator setup, which provided  $\sim 8300 \text{ km s}^{-1}$  velocity coverage and  $\sim 0.5 \text{ km s}^{-1}$  velocity resolution during the observations. Position-switching mode with beamthrows of about  $\pm 2'$  was used. Pointing and focus were checked about every two hours. The typical system temperature of the Effelsberg observations was about 46 K. The on-source time for each galaxy is about 14–47 minutes. The weather during the observations is not ideal, and the baselines of many sources are affected and induced artificial features which are hard to remove.

### 2.2. HC<sub>3</sub>N 24-23 observations with the SMT 10-m

HC<sub>3</sub>N ( $J = 24 - 23$ ) ( $\nu_{\text{rest}} = 218.324 \text{ GHz}$ ) of nine galaxies was observed in 2009 with the SMT 10-m telescope. The HPBW is about  $33''$  at  $\sim 218 \text{ GHz}$  for SMT, and a single pointing was used for each galaxy toward their central positions. We used the ALMA Sideband Separating Receiver and the Acousto-Optical Spectrometers (AOS), which have dual polarization, 970 MHz ( $\sim 1300 \text{ km s}^{-1}$ ) bandwidth and 934kHz channel spacing. Observations were carried out with the beam-switching mode with a chop throw of  $2'$  in azimuth (AZ) and a chopping frequency of 2.2 Hz. Pointing and focus were checked about every two hours by measuring nearby QSOs with strong millimeter continuum emission. The typical system temperature at 218 GHz was less than 300 K, and the on-source time for each galaxy was  $\sim 60$ –168 minutes.

### 2.3. Data Reduction

The basic parameters of our sample galaxies are listed in Table 1. The data were reduced with the CLASS program of the GILDAS<sup>1</sup> package. First, we checked each spectrum and discarded the spectra with unstable baseline. Most of the Effelsberg spectra do not have flat baselines, but over several hundred  $\text{km s}^{-1}$  near the line the baselines can still be fixed. In the SMT spectra the image signal of strong CO 2-1 in the upper sideband affect the baseline of the lower sideband and for M 82 and Arp 220 the HC<sub>3</sub>N 24-23 is contaminated. But for other galaxies the image CO line does not affect the HC<sub>3</sub>N line. Then we combined spectra with both polarizations of the same source into one spectrum. Depending on the quality of the spectral baselines, a first-order or second-order fitting was used to subtract baselines from all averaged spectra. The identifications of the transition frequencies of HC<sub>3</sub>N have made use of the NIST database *Recommended Rest Frequencies for Observed Interstellar Molecular Microwave Transitions*<sup>2</sup>.

To reduce the noise level, the spectra are smoothed to velocity resolutions  $\sim 20 - 40 \text{ km s}^{-1}$ . The velocity-integrated intensities of the HC<sub>3</sub>N line are derived from the Gaussian fit of the spectra, or integrated over a defined window if the line profiles significantly deviate from a Gaussian. The intensities are calculated using  $I = \int T_{\text{mb}} dv$ , where  $T_{\text{mb}}$  is the main beam brightness temperature. Molecular line intensity in antenna temperature ( $T_A^*$ ) is converted to main beam temperature  $T_{\text{mb}}$  via  $T_{\text{mb}} = T_A^*/\text{MBE}$ , with the main beam efficiency  $\text{MBE} = 53\%$  at 18 GHz for Effelsberg telescope, and 70% at 218 GHz for SMT during the observations. The flux density is then derived from  $T_{\text{mb}}$ , using  $S/T_{\text{mb}} = 0.59 \text{ Jy/K}$  for the Effelsberg telescope, and 24.6 Jy/K for the SMT.

## 3. Results & Discussion

The spectral measurements and estimated intensities of the HC<sub>3</sub>N lines, including RMS noise and on-source time, are listed in Table 2 (HC<sub>3</sub>N 2-1) and Table 3 (HC<sub>3</sub>N 24-23).

### 3.1. HC<sub>3</sub>N 2-1

Among the 20 galaxies observed by Effelsberg 100-m telescope, HC<sub>3</sub>N 2-1 is detected in three galaxies: IC 342, NGC 660 and

<sup>1</sup> <http://iram.fr/IRAMFR/GILDAS/>

<sup>2</sup> <http://www.nist.gov/pml/data/micro/index.cfm>

**Table 1.** The source list of the 21 galaxies observed on HC<sub>3</sub>N emission using the Effelsberg 100m and the SMT telescope. The columns are: (1) galaxy name, (2) and (3) coordinates, (4) Heliocentric velocities, (5) distances, (6) total infrared luminosities (from Sanders et al. 2003), (7) CO 1-0 linewidth (FWHM) of the galaxies, and (8) the telescope these galaxies were observed with.

Galaxy	RA (J2000)	Dec	$V_{\text{Helio}}$	Distance	$\log L_{\text{IR}}$	$\Delta V_{\text{CO}}$	Telescope
(1)	h m s	° ' "	(km s <sup>-1</sup> )	(Mpc)	( $L_{\odot}$ )	(km s <sup>-1</sup> )	(8)
NGC 520	01 24 34.9	+03 47 30.0	2281	30.22	10.91	270	Effelsberg
NGC 660	01 43 02.4	+13 38 42.0	850	12.33	10.49	280	Effelsberg
NGC 891	02 22 33.4	+42 20 57.0	528	8.57	10.27	110	Effelsberg
NGC 972	02 34 13.4	+29 18 41.0	1543	20.65	10.67	220	Effelsberg
NGC 1068	02 42 41.4	-00 00 45.0	1137	13.7	11.27	280	Effelsberg & SMT
IC 342	03 46 48.5	+68 05 46.0	31	4.60	10.17	72.8 <sup>a</sup>	Effelsberg & SMT
UGC 2855	03 48 20.7	+70 07 58.0	1200	19.46	10.75	...	Effelsberg
UGC 2866	03 50 14.9	+70 05 40.9	1232	20.06	10.68	...	Effelsberg
NGC 1569	04 30 49.0	+64 50 53.0	-104	4.60	9.49	90	Effelsberg
NGC 2146	06 18 39.8	+78 21 25.0	882	16.47	11.07	320	Effelsberg & SMT
NGC 2403	07 36 51.3	+65 36 29.9	161	3.22	9.19	90	Effelsberg
M 82	09 55 53.1	+69 40 41.0	187	3.63	10.77	150	Effelsberg & SMT
NGC 3079	10 01 57.8	+55 40 47.0	1116	18.19	10.73	380	Effelsberg
NGC 3310	10 38 45.9	+53 30 12.0	993	19.81	10.61	140	Effelsberg
M 66	11 20 15.0	+12 59 30.0	727	10.04	10.38	180	Effelsberg
IC 694	11 28 33.8	+58 33 45.0	3120	47.74	11.63	250	Effelsberg <sup>b</sup> & SMT
NGC 3690	11 28 30.8	+58 33 43.0	3120	47.74	11.32	260	Effelsberg <sup>b</sup> & SMT
Mrk 231	12 56 14.2	+56 52 25.0	12600	171.84	12.51	167	Effelsberg
Arp 220	15 34 57.1	+23 30 10.0	5352	79.90	12.21	360	Effelsberg & SMT
NGC 6240	16 52 58.9	+02 24 03.0	7160	103.86	11.85	420	SMT
NGC 6946	20 34 52.6	+60 09 12.0	53	5.32	10.16	130	Effelsberg & SMT

**Notes.** <sup>(a)</sup> for IC 342, the  $\Delta V$  is of CO 2-1 from Gao & Solomon (2004a); for other galaxies  $\Delta V$  are of CO 1-0 from Young et al. (1995). <sup>(b)</sup> The Arp 299 system (IC 694 and NGC 3690) was observed as a single pointing by the Effelsberg.

M 66 (See Figure1). This is the first report of HC<sub>3</sub>N 2-1 detections in external galaxies, although limited by the SNR (Signal to Noise Ratio) the detection rate is low.

**IC 342:** IC 342 has the strongest peak intensity ( $T_{\text{mb}} \sim 14$  mK) of HC<sub>3</sub>N 2-1 in the sample, which is about twice the strength as the HC<sub>3</sub>N(9-8) line of IC 342 detected by IRAM 30-m telescope (Aladro et al. 2011), while the line width (FWHM  $\sim 60$  km s<sup>-1</sup>) is similar to their result.

**NGC 660:** The detected HC<sub>3</sub>N 2-1 in NGC 660 has a similar linewidth (FWHM  $\sim 294.7$  km s<sup>-1</sup>) to CO 1-0 ( $\sim 280$  km s<sup>-1</sup>). While the HC<sub>3</sub>N survey by Lindberg et al. (2011) did not observe NGC 660, its 10-9 and 12-11 transitions were not detected by Costagliola et al. (2011). This difference in the detection of HC<sub>3</sub>N lines may imply that there is little warm and dense gas content in NGC 660, thus the high- $J$  HC<sub>3</sub>N lines can not be excited.

**M 66:** In M 66 HC<sub>3</sub>N 2-1 is only detected on about  $2\sigma$  level, but this is the first tentative detection of HC<sub>3</sub>N in M 66. It was not observed by Costagliola et al. (2011) nor Lindberg et al. (2011).

**non-detections:** Due to the poor quality (and probably insufficient integration time) of the HC<sub>3</sub>N 2-1 data, 16 out of 19 galaxies were not detected. Assuming their linewidth is approximate to CO 1-0 linewidth (FWHM, from Young et al. 1995), we de-

rive upper limits of the integrated intensity for each galaxy ( $2\sigma$ , where  $\sigma = \text{RMS} \sqrt{\delta V \cdot \Delta V}$ ) and show them in Table2. Note that the linewidth of HC<sub>3</sub>N is likely narrower than that of CO, and such assumption might overestimate the upper limits of integrated intensity, thus is only a rough estimate. The upper limits are in the range of  $\sim 0.3 - 1.2$  K km s<sup>-1</sup>. For those non-detection galaxies, We also stack their spectra together, weighted by the RMS level of each galaxy, to exam if a cumulated signal can be obtained (see Figure 1). Although the RMS of the the stacking HC<sub>3</sub>N 2-1 spectrum is reduced down to 0.66 mK, we do not see any signs of emission (at a resolution of 30 km s<sup>-1</sup>). Since these galaxies have similar linewidth (100–400 km s<sup>-1</sup>), we can estimate the stacked upper limit assuming a linewidth of 200 km s<sup>-1</sup>, based on the RMS (0.66 mK) of the stacked spectrum. Thus the  $2\sigma$  upper limit of these galaxies is about 0.26 K km s<sup>-1</sup>. To eliminate the possible effect induced by different linewidths of galaxies, we also tried to group the non-detection galaxies based on their CO linewidth. Galaxies with CO FWHM (Table 1) wider than 200 km s<sup>-1</sup> are stacked as one group, and other galaxies are stacked as another group. Neither group shows any signs of emission.

### 3.2. HC<sub>3</sub>N 24-23

Among the nine galaxies observed by SMT, HC<sub>3</sub>N( $J=24-23$ ) is detected in three galaxies: IC 342, NGC 1068 and IC 694 (Figure2).

**IC 342:** HC<sub>3</sub>N 24-23 of IC 342 was previously detected and measured by Aladro et al. (2011), and our observation obtains consistent result, although comparing to their observation we do not detect H<sub>2</sub>CO simultaneously. In our observations, IC 342 is the only galaxy detected in both 2-1 and 24-23 transitions. The line center and width of the two transitions are similar, considering observational uncertainties. This might imply that the two transitions have similar emitting area. And the ratio between the integrated intensities of HC<sub>3</sub>N 24-23/HC<sub>3</sub>N 2-1 is about 0.6.

**NGC 1068:** In NGC 1068, the integrated intensity of HC<sub>3</sub>N 24-23 is about 2.0 K km s<sup>-1</sup> (in  $T_{\text{mb}}$ ), which is stronger than that of HC<sub>3</sub>N 10-9 (~1.1 K km s<sup>-1</sup>) reported by Costagliola et al. (2011). It may imply that there is sufficient warm and dense gas, which is able to excite the high transition HC<sub>3</sub>N 24-23 line. Besides, it could also be affected by the strong AGN signature of this galaxy (Wang et al. 2014; Tsai et al. 2012).

**IC 694:** Previous observation only obtained upper limits of HC<sub>3</sub>N 12-11 For IC 694 (Lindberg et al. 2011). In our observations, a tentative detection in IC 694 ( $> 2\sigma$ ) is obtained. The line profile of IC 694 obviously deviates from a Gaussian, so we derive the HC<sub>3</sub>N intensity by integrating the line within a window of 400 km s<sup>-1</sup> width (Table 3).

We note that, in NGC 1068 and IC 694, HC<sub>3</sub>N 24-23 is possibly blended with H<sub>2</sub>CO 3(0,3) – 2(0,2) emission ( $f_{\nu} = 218.22219$  GHz). The upper state energy of this is para-H<sub>2</sub>CO line is about 10.5 K, which is likely to be excited in these cases. The H<sub>2</sub>CO line is shifted by 141.1 km s<sup>-1</sup> or -102 MHz from the HC<sub>3</sub>N 24-23 line, and it is unclear that how much intensity of HC<sub>3</sub>N 24-23 in NGC 1068 and IC 694 is contributed by H<sub>2</sub>CO (see Figure 2). We still lack enough data to disentangle this issue, and can only compare with other observations. For example, in the observation of M 82 by Ginard et al. (2015), they showed that near the frequency of 145 GHz, H<sub>2</sub>CO 2(0,1) – 1(0,1) is as strong as HC<sub>3</sub>N 16-15. H<sub>2</sub>CO is not detected in M 82 in 3mm band (Aladro et al. 2015). In the observations toward NGC 4418 by Aalto et al. (2007), they showed that HC<sub>3</sub>N 16-15 is blended with H<sub>2</sub>CO, and H<sub>2</sub>CO may contribute 20% of the total integrated line intensity.

**non-detections:** The spectra of M 82 and Arp 220 are seriously contaminated by the image signal of CO 2-1 from the upper sideband ( $\nu = 230$  GHz), which is strong and wide hence difficult to remove. As a consequence we could not extract the spectrum of HC<sub>3</sub>N properly. We treat the HC<sub>3</sub>N 24-23 in M 82 and Arp 220 as non-detections, and their  $2\sigma$  upper limits are also only indicative. Although not contaminated by adjacent CO image signal, HC<sub>3</sub>N 24-23 was not detected in NGC 2146, NGC 6946, NGC 3690 and NGC 6240. For these non-detection we present  $2\sigma$  upper limit of the integrated intensity of HC<sub>3</sub>N 24-23 in Table 3. Only four galaxies are not contaminated by CO image signal, thus no stacking is implemented for their HC<sub>3</sub>N 24-23 spectra.

### 3.3. Discussion: HC<sub>3</sub>N in galaxies

The HPBW of SMT and Effelsberg observations are 33'' and 46'', respectively, which should be able to cover the bulk of the sample galaxies, especially the galaxy center. Thus our observations should be able to cover the region where the majority of dense gas resides. However, with single-dish observations we can not constrain the emission size of either HC<sub>3</sub>N 2-1 or HC<sub>3</sub>N

24-23, and can not easily estimate the filling factors. Along with the large uncertainty of the emission intensities measurements, it is difficult to estimate the brightness temperature of the sample.

To better understand the excitation environment of HC<sub>3</sub>N, the effect of free-free and synchrotron emission near 18 GHz should be also taken into account, as they are more prominent than that in millimeter band that is dominated by dust thermal emission. We detect HC<sub>3</sub>N 2-1 lines in emission and not in absorption, and this may be due to the fact that the beam filling factor of the HC<sub>3</sub>N gas is higher than the radio continuum. In the high resolution radio observations towards a few nearby galaxies (Tsai et al. 2006), it is found that compact radio sources contribute 20% – 30% of the total 2 cm (15 GHz) emission from the central kiloparsec of these galaxies. In contrast, the distribution of gas with moderate critical density such as HC<sub>3</sub>N 2-1 is likely more diffuse.

Comparing to other dense molecular gas tracers such as the popular HCN and HCO<sup>+</sup>, HC<sub>3</sub>N is generally optically thin in galaxies owing to its relatively low abundance, which makes it an ideal dense gas tracer for calculating the column density and/or mass of molecular hydrogen content of galaxies. In the observations by Lindberg et al. (2011) and Costagliola et al. (2011) a low detection rate of HC<sub>3</sub>N was reported and was explained as the intrinsically faint emission of HC<sub>3</sub>N, and our stacked result also implies that the HC<sub>3</sub>N is quite weak in the non-detected galaxies ( $2\sigma$  upper limit = 0.14 K km s<sup>-1</sup>), which is also in favor of this explanation. The non-detection in M 82 is consistent with the low abundance of HC<sub>3</sub>N in M 82 suggested by Aladro et al. (2011), that HC<sub>3</sub>N traces a nascent starburst of galaxy, and it can be easily destroyed by the UV radiation in PDRs, which is ubiquitous in active galaxies.

In very recent line surveys of a few local active galaxies (AGN and/or Starbursts, Aladro et al. 2015; Costagliola et al. 2015), several HC<sub>3</sub>N transitions in 3mm band (HC<sub>3</sub>N  $J=10-9$ ,  $J=11-10$  and  $J=12-11$ ) were detected. The ALMA observations by Costagliola et al. (2015) even reported the HC<sub>3</sub>N  $J=32-31$  rotational transition, and some of the vibrationally excited HC<sub>3</sub>N lines. The latest high resolution line surveys in a few very nearby galaxies (Meier & Turner 2005, 2012) and Meier et al. (2014, 2015) show that, the derived HC<sub>3</sub>N abundances (on ~ 100 pc, roughly GMC scales) are about several 10<sup>-10</sup> (relative to H<sub>2</sub>), which is about an order of magnitude lower than the abundance of HCN and some other molecules.

The results in Aladro et al. (2015) show that, the HC<sub>3</sub>N fractional abundance is generally several times lower than that of HCN, HCO<sup>+</sup> and CS. And comparing to other AGN or starburst galaxies in their sample, HC<sub>3</sub>N abundance is significantly higher in the two ULIRGs Arp 220 and Mrk 231, implying it is suited for studying the activity of ULIRGs. Besides, there was no obvious evidence of the affection by AGN on the intensity of HC<sub>3</sub>N. Four galaxies in our sample (NGC 1068, M 82, Mrk 231 and Arp 220) were also studied in Aladro et al. (2015). We compare our data with their results, and the HC<sub>3</sub>N spectra of Mrk 231 and NGC 1068 from Aladro et al. (2015) are shown in Figure 1 and 2, to be compared with the non-detection of HC<sub>3</sub>N 2-1 in Mrk 231, and the detection of HC<sub>3</sub>N 24-23 in NGC 1068, respectively. Their results show that, in 3mm band, the intensities between the three transitions of HC<sub>3</sub>N (10-9, 11-10 and 12-11) differ not too much, and the peak temperature ( $T_{\text{mb}}$ ) of HC<sub>3</sub>N are ~ 4 mK for NGC 1068, ~ 11 mK for M 82, and ~ 1.1 – 1.7 mK for Mrk 231, and ~ 10 mK for Arp 220. In our results, the detection of HC<sub>3</sub>N 24-23 in NGC 1068 shows a peak  $T_{\text{mb}} \sim 7$  mK, while the non-detection of HC<sub>3</sub>N 2-1 in Mrk 231 and Arp 220 show that, the RMS we have (~ 4–6 mK) might not be low

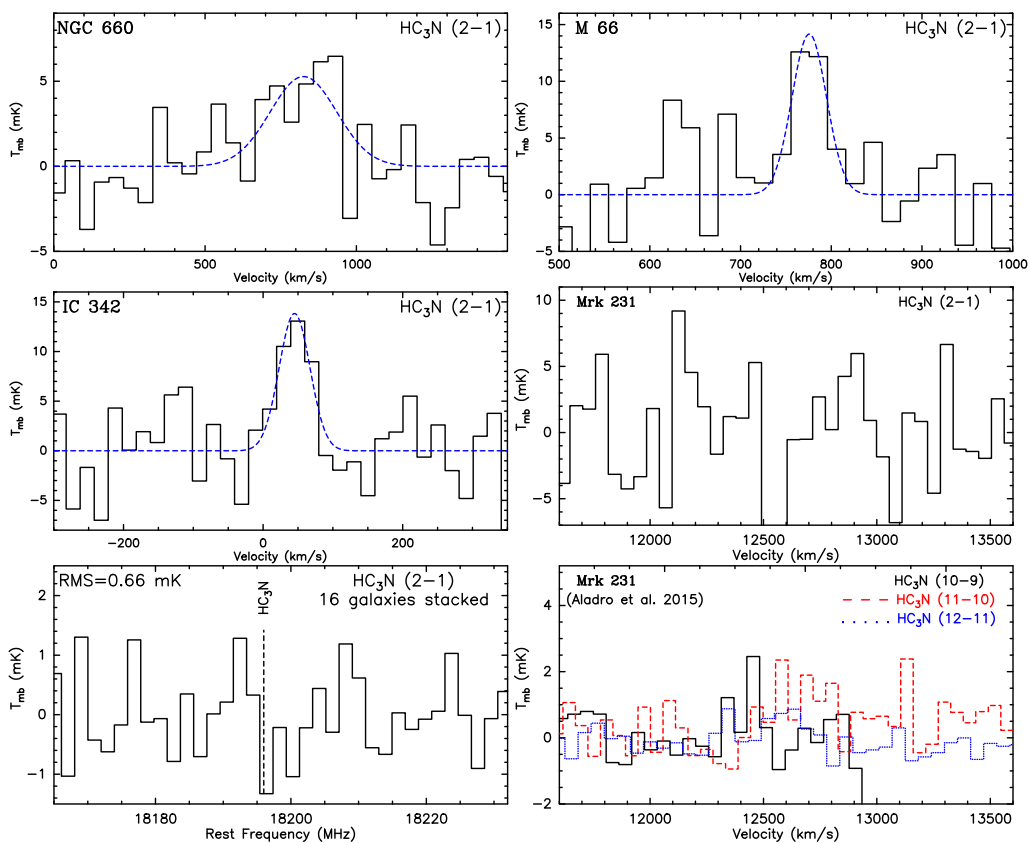


**Fig. 1.** Spectra of the detected HC<sub>3</sub>N( $J=2-1$ ) in NGC 660, M 66, IC 342 by the Effelsberg. At the bottom row also shows the stacked spectra and the spectra of Mrk 231 from Aladro et al. (2015). Blue dashed lines are the Gaussian fit of the HC<sub>3</sub>N 2-1 lines. Temperature scale is  $T_{\text{mb}}$  in mK. A colour version of this figure is available in the online journal.

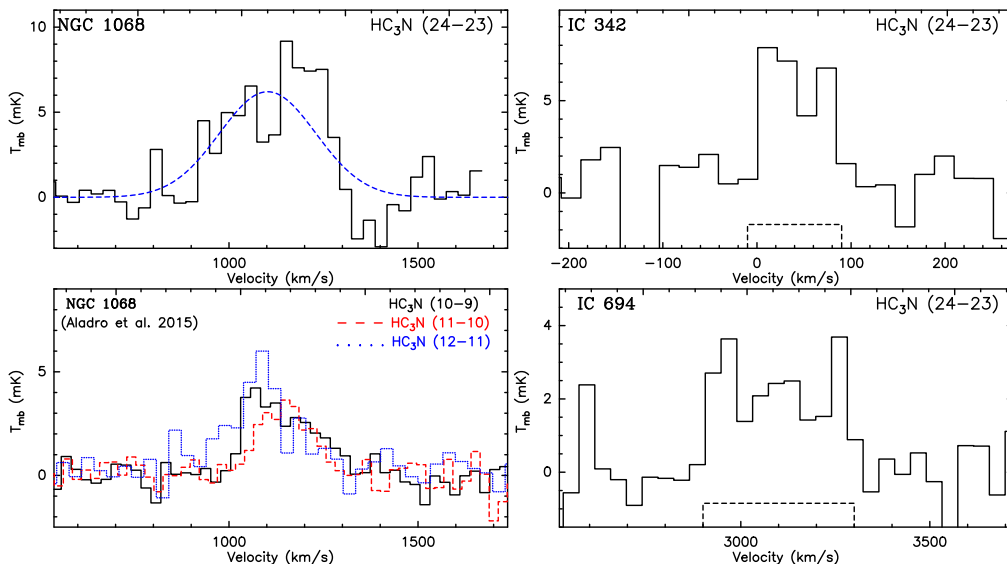


**Fig. 2.** Spectra of detected HC<sub>3</sub>N( $J=24-23$ ) in NGC 1068, IC 342 and IC 694 by the SMT. At the bottom left also shows the spectra of NGC 1068 from Aladro et al. (2015) for comparison. Blue dashed line is the Gaussian fit. Note that in IC 694 it is difficult to distinguish the HC<sub>3</sub>N emission from the possibly blended H<sub>2</sub>CO lines. Temperature scale is  $T_{\text{mb}}$  in mK. A colour version of this figure is available in the online journal.

enough to detection the HC<sub>3</sub>N lines. Here we conclude that, besides the low abundance of HC<sub>3</sub>N, insufficient integration time and not ideal observing conditions are the main cause for the low detection rate of HC<sub>3</sub>N.

It would be interesting to compare the intensity ratios between HC<sub>3</sub>N and other dense gas tracers, such as HCN and

HCO<sup>+</sup>. We list the ratio between the flux density of HC<sub>3</sub>N and HCN 1-0 in Table 2 and 3, respectively. Because the data quality of this work is not good enough for us to present an accurate estimate on the HC<sub>3</sub>N flux density, the ratios are only tentative. We see a large variation in the ratios, which could be an evidence of the essentially large variation of HC<sub>3</sub>N luminosities

**Table 2.** HC<sub>3</sub>N 2-1 spectral measurements. All the temperature scales are  $T_{\text{mb}}$ . The columns are: (1) galaxy name, (2) on-source time for each galaxy, (3) RMS noise of the smoothed spectrum, (4) velocity resolution of the smoothed spectrum, (5) linewidth (FWHM) of the Gaussian fit of the line (if available), (6) HC<sub>3</sub>N emission line center, (7) Integrated intensity (and errors) of HC<sub>3</sub>N 2-1 emission. For those non-detections,  $2\sigma$  upper limits are presented (see text in Section 3.1), (8) Integrated flux density, and (9) flux density ratio between HC<sub>3</sub>N 2-1 and HCN 1-0.

Source	On-time (min)	RMS (mK)	$\delta V$ (km s <sup>-1</sup> )	$\Delta V$ (km s <sup>-1</sup> )	$V_0$ (km s <sup>-1</sup> )	$I(\text{HC}_3\text{N})$ (K km s <sup>-1</sup> )	$S(\text{HC}_3\text{N})$ (Jy km s <sup>-1</sup> )	$\frac{\text{HC}_3\text{N } 2-1}{\text{HCN } 1-0}$
(1)	(2)	(3)	(4)	(5)	(6)	(7)	(8)	(9)
NGC 660	28	4.2	32.2	260.7 (90.6)	825 (36)	1.47 (0.40)	0.86 (0.24)	$\sim 0.034^a$
IC 342	20	6.5	20.1	52.0 (12.9)	45 (6)	0.77 (0.18)	0.45 (0.11)	$\sim 0.005^b$
M 66	18	7.0	20.1	44.8 (17.7)	775 (7)	0.68 (0.21)	0.4 (0.12)	$\sim 0.114^c$
NGC 520	14	5.7	...	...	...	< 1.02	< 0.6	< 0.087 <sup>d</sup>
NGC 891	30	2.3	...	...	...	< 0.26	< 0.15	< 0.033 <sup>e</sup>
NGC 972	33	3.8	...	...	...	< 0.61	< 0.36	...
NGC 1068	25	4.0	...	...	...	< 0.73	< 0.43	< 0.013 <sup>f</sup>
UGC 2855	23	4.9	...	...	...	< 0.76*	< 0.45	...
UGC 2866	22	3.6	...	...	...	< 0.56*	< 0.33	...
NGC 1569	33	3.0	...	...	...	< 0.31	< 0.18	...
NGC 2146	24	3.4	...	...	...	< 0.67	< 0.39	< 0.021 <sup>e</sup>
NGC 2403	30	3.2	...	...	...	< 0.33	< 0.19	...
M 82	26	5.5	...	...	...	< 0.73	< 0.43	< 0.011 <sup>e</sup>
NGC 3079	19	5.5	...	...	...	< 1.17	< 0.69	< 0.225 <sup>e</sup>
NGC 3310	36	2.3	...	...	...	< 0.29	< 0.17	...
IC 694+NGC3690	47	4.2	...	...	...	< 0.72	< 0.42	< 0.158 <sup>g</sup>
Mrk 231	44	6.4	...	...	...	< 0.91	< 0.54	< 0.191 <sup>g</sup>
Arp 220	26	4.5	...	...	...	< 0.94	< 0.55	< 0.069 <sup>h</sup>
NGC 6946	28	5.1	...	...	...	< 0.64	< 0.38	< 0.018 <sup>e</sup>

**Notes.** <sup>(a)</sup> The upper limits of the two galaxies are derived assuming a 200 km s<sup>-1</sup> linewidth.

HCN 1-0 data from: <sup>(a)</sup> Baan et al. (2008); <sup>(b)</sup> Nguyen et al. (1992); <sup>(c)</sup> Krips et al. (2008); <sup>(d)</sup> Solomon et al. (1992); <sup>(e)</sup> Gao & Solomon (2004a); <sup>(f)</sup> Aladro et al. (2015); <sup>(g)</sup> Jiang et al. (2011); <sup>(h)</sup> Wang et al. (2016).

**Table 3.** HC<sub>3</sub>N 24-23 spectral measurements. Columns are the same as Table 2.

Source	On-time (min)	RMS (mK)	$\delta V$ (km s <sup>-1</sup> )	$\Delta V$ (km s <sup>-1</sup> )	$V_0$ (km s <sup>-1</sup> )	$I(\text{HC}_3\text{N})$ (K km s <sup>-1</sup> )	$S(\text{HC}_3\text{N})$ (Jy km s <sup>-1</sup> )	$\frac{\text{HC}_3\text{N } 24-23}{\text{HCN } 1-0}$
(1)	(2)	(3)	(4)	(5)	(6)	(7)	(8)	(9)
NGC 1068	121	1.2	39.1	257.3 (24.0) <sup>a</sup>	1102 (13)	2.03 (0.18)	49.9 (4.4)	$\sim 0.59$
IC 342	132	2.7	20.9	100 <sup>b</sup>	43	0.47 (0.12)	11.6 (3.0)	$\sim 0.12$
IC 694	127	0.87	41.7	400 <sup>b</sup>	3095	0.90 (0.11)	22.1 (2.7)	$\sim 2.76$
NGC 2146	115	1.01	20.9	320 <sup>c</sup>	...	< 0.17	4.2	< 0.26
M 82	60	3.0	20.9	150 <sup>c</sup>	...	< 0.34	8.4	< 0.26
NGC 3690	139	0.73	42.0	260 <sup>c</sup>	...	< 0.15	3.7	< 1.27
ARP 220	162	0.75	39.1	420 <sup>c</sup>	...	< 0.19	4.7	< 0.48
NGC 6240	97	0.92	20.1	420 <sup>c</sup>	...	< 0.17	4.2	< 1.15
NGC 6946	168	1.76	21.0	130 <sup>c</sup>	...	< 0.18	4.4	< 0.26

**Notes.** <sup>(a)</sup> FWHM from the Gaussian fitting and error. <sup>(b)</sup> line window (full width) used to derived the integrated intensity. <sup>(c)</sup> CO width from Young et al. (1995) that are used to derived the upper limits.

among galaxies. In the HC<sub>3</sub>N survey by Lindberg et al. (2011), ratios like HC<sub>3</sub>N/HCN were used to compare HC<sub>3</sub>N between galaxies. Based on that ratio, IC 342 and M 82 were classified as HC<sub>3</sub>N-luminous galaxies. In our observation we detect both HC<sub>3</sub>N 2-1 and HC<sub>3</sub>N 24-23 in IC 342, but neither HC<sub>3</sub>N transition is detected in M 82. On the other hand, we obtained HC<sub>3</sub>N 24-23 detections in NGC 1068 which were classified as a HC<sub>3</sub>N-poor galaxy in Lindberg et al. (2011). In the sample of some nearby galaxies observed by Aladro et al. (2015), the ratio between the peak temperature ( $T_{\text{mb}}$ ) of HC<sub>3</sub>N/HCN or

HC<sub>3</sub>N/HCO<sup>+</sup> also show large variance. In NGC 253 and M 82, HC<sub>3</sub>N 10-9 is only  $\sim 1/20$  as strong as HCO<sup>+</sup> 1-0, while in Arp 220 HC<sub>3</sub>N 10-9 is nearly as strong as HCO<sup>+</sup> 1-0. In our results such line ratios also show large diversity. It is not yet clear how to interpret the ratio between HC<sub>3</sub>N and other molecular lines, and more data of HC<sub>3</sub>N in different transitions would be helpful to disentangle its properties in different types of galaxies.

Our observations and other works have presented detection of HC<sub>3</sub>N emission lines from near 18 GHz up to  $\sim 292$  GHz. The newly commissioned Tianma 65 m telescope in Shanghai,

China, is able to observe low transition HC<sub>3</sub>N emission, and has great potential for further HC<sub>3</sub>N 2-1 surveys for large sample of galaxies.

#### 4. Summary

We carry out single-dish observations towards a sample of nearby gas-rich galaxies with the Effelsberg telescope and the Submillimeter Telescope. This is the first measurements of HC<sub>3</sub>N 2-1 in a relatively large sample of external galaxies. Our results include:

1. HC<sub>3</sub>N( $J=2-1$ ) ( $\nu = 18.196$  GHz) was observed with the 100-m telescope in 20 galaxies and only three galaxies are detected ( $> 3\sigma$ ): IC 342, M 66 and NGC 660. This is the first measurements of HC<sub>3</sub>N 2-1 reported in external galaxies, and the first HC<sub>3</sub>N detection in M 66. We stack the spectra of those non-detections yet there is still no sign of HC<sub>3</sub>N emission. The  $2\sigma$  upper limit of HC<sub>3</sub>N intensity from the stacked spectrum is about  $0.12 \text{ K km s}^{-1}$ .
2. HC<sub>3</sub>N( $J=24-23$ ) ( $\nu = 218.324$  GHz) was observed in nine galaxies with the SMT, and it is detected in three galaxies: IC 342, IC 694 and NGC 1068.
3. IC 342 is the only galaxies detected in both HC<sub>3</sub>N 2-1 and HC<sub>3</sub>N 24-23 transitions in our observations, and the two transitions have similar line center and width, suggesting a similar emitting area. The ratio of integrated intensity of HC<sub>3</sub>N 24-23/HC<sub>3</sub>N 2-1 is about 0.82. Due to the contamination of CO 2-1 image signal in the upper sideband, M 82 and Arp 220 are treated as non-detection of HC<sub>3</sub>N 24-23.
4. The ratios between HC<sub>3</sub>N and HCN, HCO<sup>+</sup> show a large variance among the galaxies with HC<sub>3</sub>N detections, implying different behavior of the molecular lines in galaxies. More sample are needed to better understand the relationship between HC<sub>3</sub>N and other molecules.

*Acknowledgements.* We thank the staff of the Effelsberg telescope and the SMT for their kind help and support during our observations. This project is funded by China Postdoctoral Science Foundation (grant 2015M580438), National Natural Science Foundation of China (grant 11420101002, 11311130491, 11590783 and 11603075), and the CAS Key Research Program of Frontier Sciences. This research has made use of NASA's Astrophysics Data System, and the NASA/IPAC Extragalactic Database (NED), which is operated by the Jet Propulsion Laboratory, California Institute of Technology, under contract with the National Aeronautics and Space Administration.

## References

- Aalto, S., Monje, R., & Martín, S. 2007, *A&A*, 475, 479 2, 4
- Aladro, R., Martín, S., Riquelme, D., et al. 2015, *A&A*, 579, A101 2, 4, 5, 6
- Aladro, R., Martín-Pintado, J., Martín, S., Mauersberger, R., & Bayet, E. 2011, *A&A*, 525, A89 1, 2, 3, 4
- Baan, W. A., Henkel, C., Loenen, A. F., Baudry, A., & Wiklind, T. 2008, *A&A*, 477, 747 6
- Baan, W. A., Loenen, A. F., & Spaans, M. 2014, *MNRAS*, 445, 3331 1
- Costagliola, F. & Aalto, S. 2010, *A&A*, 515, A71 2
- Costagliola, F., Aalto, S., Rodríguez, M. I., et al. 2011, *A&A*, 528, A30 1, 2, 3, 4
- Costagliola, F., Sakamoto, K., Müller, S., et al. 2015, *Astronomy and Astrophysics*, 582, A91 4
- Evans, II, N. J. 1999, *ARA&A*, 37, 311 1
- Fukui, Y. & Kawamura, A. 2010, *ARA&A*, 48, 547 1
- Gao, Y. & Solomon, P. M. 2004a, *ApJS*, 152, 63 2, 3, 6
- Gao, Y. & Solomon, P. M. 2004b, *ApJ*, 606, 271 2
- Ginard, D., Fuente, A., García-Burillo, S., et al. 2015, *A&A*, 578, A49 4
- Greve, T. R., Papadopoulos, P. P., Gao, Y., & Radford, S. J. E. 2009, *ApJ*, 692, 1432 1
- Henkel, C., Baan, W. A., & Mauersberger, R. 1991, *Astron. Astrophys. Rev.*, 3, 47 1
- Henkel, C., Schilke, P., & Mauersberger, R. 1988, *A&A*, 201, L23 2
- Irvine, W. M., Goldsmith, P. F., & Hjalmarsen, A. 1987, in *Astrophysics and Space Science Library*, Vol. 134, *Interstellar Processes*, ed. D. J. Hollenbach & H. A. Thronson, Jr., 561–609 2
- Jiang, X., Wang, J., & Gu, Q. 2011, *MNRAS*, 418, 1753 6
- Krips, M., Neri, R., García-Burillo, S., et al. 2008, *ApJ*, 677, 262 6
- Lindberg, J. E., Aalto, S., Costagliola, F., et al. 2011, *A&A*, 527, 17 2, 3, 4, 6
- Meier, D. S. & Turner, J. L. 2005, *ApJ*, 618, 259 2, 4
- Meier, D. S. & Turner, J. L. 2012, *ApJ*, 755, 104 1, 2, 4
- Meier, D. S., Turner, J. L., & Beck, S. C. 2014, *ApJ*, 795, 107 1, 2, 4
- Meier, D. S., Turner, J. L., & Schinnerer, E. 2011, *AJ*, 142, 32 2
- Meier, D. S., Walter, F., Bolatto, A. D., et al. 2015, *ApJ*, 801, 63 4
- Nguyen, Q.-R., Jackson, J. M., Henkel, C., Truong, B., & Mauersberger, R. 1992, *ApJ*, 399, 521 6
- Sanders, D. B., Mazzarella, J. M., Kim, D.-C., Surace, J. A., & Soifer, B. T. 2003, *AJ*, 126, 1607 2, 3
- Solomon, P. M., Downes, D., & Radford, S. J. E. 1992, *ApJ*, 387, L55 6
- Suzuki, H., Yamamoto, S., Ohishi, M., et al. 1992, *ApJ*, 392, 551 1
- Tsai, C.-W., Turner, J. L., Beck, S. C., et al. 2006, *AJ*, 132, 2383 4
- Tsai, M., Hwang, C.-Y., Matsushita, S., Baker, A. J., & Espada, D. 2012, *ApJ*, 746, 129 4
- Turner, B. E. 1971, *ApJ*, 163, L35 1
- Viti, S., García-Burillo, S., Fuente, A., et al. 2014, *A&A*, 570, A28 1
- Wang, J., Zhang, Z., & Shi, Y. 2011, *MNRAS*, 416, L21 2
- Wang, J., Zhang, Z.-Y., Qiu, J., et al. 2014, *ApJ*, 796, 57 4
- Wang, J., Zhang, Z.-Y., Zhang, J., Shi, Y., & Fang, M. 2016, *MNRAS*, 455, 3986 6
- Young, J. S., Xie, S., Tacconi, L., et al. 1995, *ApJS*, 98, 219 3, 6
- Zhang, Z.-Y., Gao, Y., Henkel, C., et al. 2014, *ApJ*, 784, L31 2